Upper bounds of lateral tire slip loss minimization during daily driving using torque vectoring

Juliette Torinsson[1,2], Mats Jonasson[2], Derong Yang[1] & Bengt Jacobson[2]

[1] Department of Vehicle Energy and Motion Control, Volvo Car Corporation, Gothenburg, Sweden
[2] Department of Vehicle Engineering and Autonomous Systems, Chalmers, Gothenburg, Sweden
E-mail: juliette.torinsson@volvocars.com

Previous research has shown the potential of reducing the power consumption during cornering using torque vectoring. However, the results are either closely related to the efficiencies of the electric motors used to realize the direct yaw moment, or not put into context of the total energy of transportation. In this study, the effect of direct yaw moment on lateral tire slip power loss is investigated and put into relation with the total power consumption in mild steady state cornering for four different levels of understeer. An expression for the optimal direct yaw moment is derived and is validated in simulation using a high fidelity CarMaker model where it was found that up to 2.9 % in lateral tire slip loss can be reduced depending on the understeer gradient. However, this reduction is negated by an increase in longitudinal tire slip losses generated through torque vectoring. Minimizing the total tire slip losses, up to 0.16 % could be saved considering the total power consumption of the vehicle during the maneuver.

Topics / Vehicle Dynamics Theory, Electrified Vehicles.

1. INTRODUCTION

Energy efficiency in electric vehicles can be improved through distribution of wheel torque that minimizes generated power losses in the drivetrain and tires [1–3]. In the longitudinal direction, the distribution between the front and the rear motors is studied, but during cornering the distribution between the vehicle sides, i.e. torque vectoring, can be used to minimize power losses. In [3] they found that to minimize the tire power losses, the tire slip velocity vectors should be equal on all four wheels. Focusing on the lateral tire slip, this indicates that a neutral steering tendency is desired for reduced lateral tire slip power losses. This is supported by [4–7] where the power consumption of understeered vehicles is improved by destabilizing yaw moments. In [7], experiments were conducted with a four-motor electric vehicle where the total energy consumption reduced by 5.4 % for 2 m/s^2 in lateral acceleration and up to 12.3 % for 8 m/s^2. It is, however, unclear how much of this improvement is due to minimization of lateral tire slip power loss and how much is due to the power consumption of the electric motors. Furthermore, according to [8] normal driving does not exceed 3 m/s^2, making driving scenarios using higher lateral accelerations less relevant for energy efficient daily driving. This work aims to provide a deeper understanding of how lateral tire slip power loss is affected by the understeer level of the vehicle, and how torque vectoring can be used to reduce it for normal driving scenarios. An optimization problem is formulated where the objective is to minimize lateral tire slip power losses through a direct yaw moment. The effect on the lateral tire slip power losses will then be put into context with the longitudinal tire slip power losses generated through torque vectoring and the total power consumption of the vehicle during the maneuver. Power losses generated by the electric drivetrain will be excluded from the study as the aim is to see the potential of minimizing tire slip power losses unbiased by the type of electric machine used. It will, however, be used for comparison to put the tire power losses into context. The study will consider mild lateral accelerations, as higher lateral accelerations are a small part of normal driving.

2. PROBLEM DEFINITION

The first part of this work concerns only the lateral tire slip losses since it is desired to see the maximum potential of minimizing these losses through torque vectoring, and how this potential is affected by the understeer gradient. As it has been indicated in previous research that a neutral steering behaviour seems to be desired for reduced power consumption during cornering, a front wheel steered, steady state one-track model is used to derive the equation for required steering angle including the effect of the understeer gradient and a direct yaw moment. An expression for the lateral tire slip losses will then be derived and used in an optimization formulation where the optimal direct yaw moment required to minimize the lateral tire slip losses is found. By inserting this optimal direct yaw moment into the equation for steering angle, it cancels the effect of

the understeer gradient and makes the vehicle neutral steered.

The lateral tire slip loss can vary for two vehicles with the same understeer gradient depending on the tire stiffnesses and the axle distance to center of gravity, making it challenging to conclude the effect of the understeer gradient alone on the lateral tire slip losses. A neutralsteered vehicle, for example, can have higher lateral tire slip losses than an understeered vehicle if the lateral tire stiffnesses are lower. However, using the same vehicle one can conclude the potential for reducing the lateral tire slip loss for a more or less understeered vehicle using a direct yaw moment, which is what is being investigated in this work.

2.1 One-track vehicle model

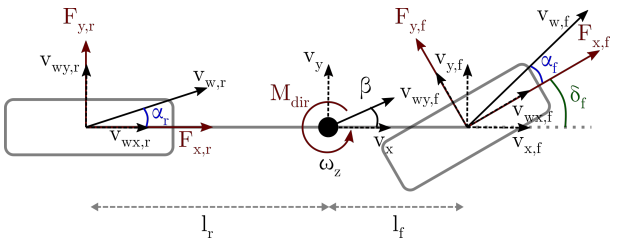

Fig. 1: One-track vehicle model

The steady state equations of motion for a one-track model can be derived from figure 1. Small angles are assumed here, meaning $\cos\delta \approx 1, \sin\delta \approx \delta$ and $\delta^2 \approx 0$.

$$-mv_y\omega_z = F_{x,f} + F_{x,r} - F_{y,f}\delta_f \quad (1)$$

$$mv_x\omega_z = F_{y,f} + F_{y,r} + F_{x,f}\delta_f \quad (2)$$

$$0 = F_{y,f}l_f - F_{y,r}l_r + F_{x,f}l_f\delta + M_{dir} \quad (3)$$

Since the one-track model merges each axis into one single wheel, torque vectoring is realized through an externally applied direct yaw moment M_{dir}. Using a linear tire model with small angle approximation.

$$F_{y,j} = -C_{t,j}\alpha_j \quad (4)$$

$$\alpha_j = \frac{v_{y,j}}{v_{x,j}} - \delta_j \quad (5)$$

where $C_{t,j}$ is the lateral tire stiffness on axle $j \in \{f, r\}$. Combining (1)-(5), assuming $\omega_z \approx \frac{v_x}{R_p}$, $\frac{F_{x,f}}{C_{t,f}} \approx 0$, $a_y = \frac{v_x^2}{R_p}$, and defining the understeer gradient

$$K_{us} = \frac{m\left(C_{t,r}l_r - C_{t,f}l_f\right)}{C_{t,f}C_{t,r}L} \quad (6)$$

the wheel angle δ_f can be expressed as a function of understeer gradient K_{us} and direct yaw moment M_{dir}.

$$\delta_f \approx \frac{L}{R_p} + K_{us}a_y - \frac{(C_{t,f} + C_{t,r})}{C_{t,f}C_{t,r}L}M_{dir} \quad (7)$$

A neutral steered vehicle is defined as $\delta_f = \frac{L}{R_p}$, meaning that the direct yaw moment that makes the vehicle neutralsteered can be found by letting the sum of the second and third term on the right hand side of (7) equal to 0.

$$K_{us}a_y = \frac{(C_{t,f} + C_{t,r})}{C_{t,f}C_{t,r}L}M_{dir} \quad (8)$$

$$M_{dir} = \frac{C_{t,f}C_{t,r}L}{(C_{t,f} + C_{t,r})}K_{us}a_y \quad (9)$$

The direct yaw moment required to make the vehicle neutralsteered is thus depedent on the lateral tire stiffness, the understeer gradient and the lateral acceleration.

2.2 Lateral tire slip power loss

The total tire slip power loss is modelled as

$$P_{s,tot} = \sum_{i=1}^{4}\left(F_{x,i}\left(\omega_i r_{e,i} - v_{wx,i}\right) - F_{y,i}v_{wy,i}\right) \quad (10)$$

where $r_{e,i}$ is the effective rolling radius of tire i. The first and second term represent the power loss due to longitudinal (P_{sx}) and lateral slip (P_{sy}) respectively.

Assuming the same slip between the tires on the front and rear axle (α_f and α_r), the same lateral tire stiffness ($C_{t,f}$ and $C_{t,r}$), and $v_{wx,i} \approx v_{x,i}$, the lateral tire slip loss can be rewritten as a function of lateral tire force according to

$$P_{sy} = \left(\frac{F_{y,f}^2}{C_{t,f}} + \frac{F_{y,r}^2}{C_{t,r}}\right)v_x \quad (11)$$

2.3 Minimizing P_{sy}

The optimization problem concerning the minimization of lateral tire slip power loss during steady state cornering can be formulated in the following way, assuming that no longitudinal tire force is applied.

$$\min_{F_{y,f},F_{y,r},M_{dir}} \quad \left(\frac{F_{y,f}^2}{C_{t,f}} + \frac{F_{y,r}^2}{C_{t,r}}\right)v_x \quad (12a)$$

$$\text{subject to:} \quad F_{y,f} + F_{y,r} = ma_y \quad (12b)$$

$$F_{y,f}l_f - F_{y,r}l_r + M_{dir} = 0 \quad (12c)$$

with the lateral tire forces $F_{y,f}$, $F_{y,r}$ and the direct yaw moment M_{dir} as optimization variables. Due to the quadratic nature of the optimization problem, it can be written in the form of a quadratic program.

$$\min_x \quad x^TPx + k^Tx \quad (13a)$$

$$\text{subject to:} \quad Ex = d \quad (13b)$$

where

$$x = \begin{bmatrix} F_{y,f} \\ F_{y,r} \\ M_{dir} \end{bmatrix} \quad P = \begin{bmatrix} \frac{1}{C_{t,f}}v_x & 0 & 0 \\ 0 & \frac{1}{C_{t,r}}v_x & 0 \\ 0 & 0 & 0 \end{bmatrix} \quad k = \begin{bmatrix} 0 \\ 0 \\ 0 \end{bmatrix}$$

$$d = \begin{bmatrix} ma_y \\ 0 \end{bmatrix} \quad E = \begin{bmatrix} 1 & 1 & 0 \\ l_f & -l_r & 1 \end{bmatrix}$$

Since only equality constraints are used in the problem definition, an analytical optimal solution can be found

$$\begin{bmatrix} x^* \\ \lambda^* \end{bmatrix} = \begin{bmatrix} P & E^T \\ E & 0 \end{bmatrix}^{-1} \begin{bmatrix} -k \\ d \end{bmatrix} \tag{14}$$

where

$$F^*_{y,j} = \frac{C_{t,j}}{C_{t,f} + C_{t,r}} m a_y \tag{15}$$

$$M^*_{dir} = \frac{(C_{t,r} l_r - C_{t,f} l_f)}{C_{t,f} + C_{t,r}} m a_y \tag{16}$$

Using a linear tire model (4) gives us the optimal lateral tire slip angles,

$$\alpha^*_f = \alpha^*_r = -\frac{1}{C_{t,f} + C_{t,r}} m a_y \tag{17}$$

From (17) it can be seen that the optimal lateral tire slip angles depend on the sum of the lateral tire stiffness, the mass of the vehicle and the lateral acceleration. Furthermore, it is also seen that the lateral slip angles should be the same on the front and the rear axle, indicating a neutral steering behaviour. Inserting M^*_{dir} into (7) yields

$$\begin{aligned} \delta_f =& \frac{L}{R_p} + K_{us} a_y - \\ & \frac{(C_{t,f} + C_{t,r})}{C_{t,f} C_{t,r} L} \cdot \left(\frac{(C_{t,r} l_r - C_{t,r} l_r)}{(C_{t,f} + C_{t,r})} m a_y \right) \\ =& \frac{L}{R_p} \end{aligned} \tag{18}$$

Hence, a vehicle that is made neutralsteered through a direct yaw moment generates the lowest lateral tire slip loss.

3. SIMULATION

A simulation study was performed in IPG CarMaker to validate the derived optimal yaw moment for four configurations with different levels of understeer; two oversteered and two understeered. The different understeer gradients were realized by tuning the lateral tire stiffness. The test case consists of steady state driving in a constant radius with a lateral acceleration of 2 m/s^2. The radius of the circle is limited to 40 m to match the skid pad present at Hällered proving ground to be able to connect the results obtained through simulation to experimental tests in the future. Hence, the velocity is 32.2 km/h. A range of direct yaw moments $M_{dir} \in [-1500, 1500]$ Nm were realized through torque vectoring and the lateral tire slip loss was recorded for the different understeer configurations.

3.1 One-track vehicle model

A conventional SUV vehicle model is used in this work with corresponding vehicle parameters presented in table 1. The understeer gradient is calculated according to (6), and the different understeer levels are realized through the tuning of lateral tire stiffness on the front and rear axle, which is presented in table 2.

Table 1: Vehicle parameters.

Vehicle parameter	Value	Unit
Mass, m	2443	[kg]
Inertia, I_{zz}	5619	[kgm^2]
CoG distance to front axle, l_f	1.45	[m]
CoG distance to rear axle, l_r	1.54	[m]
Steer ratio, i_{st}	16	[-]

The sum of the lateral tire stiffness is kept the same while the balance between front and rear stiffness is altered, i.e. $C_{t,f} = \gamma C_{tot}$, $C_{t,r} = (1-\gamma) C_{tot}$ where $C_{tot} = C_{t,f} + C_{t,r}$ and γ is tuned. The one-track model is used to calculate the optimal direct yaw moments according to (16) with the obtained lateral tire stiffnesses.

Table 2: One-track model: Understeer configurations.

K_{us} [rad/(m/s^2)]	$C_{t,f}$ [N/rad]	$C_{t,r}$ [N/rad]
-0.0018	2.37e+05	1.67e+05
-0.0009	2.24e+05	1.81e+05
0.0009	1.93e+05	2.11e+05
0.0018	1.78e+05	2.26e+05

3.2 CarMaker model

The CarMaker model includes four permanent magnet synchronous motors to realize torque vectoring where the torque is divided equally between the front and rear motors on each side. The electric losses have been omitted from the total power consumption to not bias the results with the type of electric machine used. Similiar to the one-track model, the sum of the lateral tire stiffness on front and rear tires was kept the same while the balance between the front and rear is altered to realize the different understeer gradients. In CarMaker, the lateral stiffness of a tire can be altered by the scale factor LKY when using a Magic Formula tire file. The longitudinal and lateral tire slip power losses are predefined signals in CarMaker.

The definition for understeer gradient using (6) is numerically sensitive to variations in lateral stiffness since the numerator consists of two very large values ($C_{t,f}$ and $C_{t,r}$) that are multiplied with in comparison very small values (l_f and l_r), making it hard to implement as in reality the exact value of lateral tire stiffness is hard to estimate. Thus, a different way of calculating the understeer gradient in CarMaker is used. A second definition of the understeer gradient can be derived from (7) with $M_{dir} = 0$ defined below.

$$K_{us} = \frac{1}{v_x} \left(\frac{\delta_f}{\omega_z} - \frac{L}{v_x} \right) \tag{19}$$

In the common definition of understeer gradient, δ_f is derived from the steering wheel angle δ_{swa} rather than the wheel angle δ_f. However, the CarMaker model includes suspension effects such as sideforce

Table 3: Lateral tire slip loss at M^*_{dir} for different understeer gradients.

K_{us} [rad/(m/s^2)]	M^*_{dir} [Nm]	P_{sy}@M^*_{dir} [W]	P_{sy} decrease compared to $M_{dir} = 0$ [%]
-0.0018	-1047	507.0	2.91
-0.0009	-551	506.8	0.94
0.0009	555	505.7	0.37
0.0018	1097	508.5	1.82

understeer which will affect the understeer gradient when δ_{swa} is used which is not represented in the one-track model. Thus, the definition used here includes the average wheel angle between the left and right tire in order to replicate the one-track model's understeer gradient, in the CarMaker model, as close as possible.

4. RESULTS

The effect of torque vectoring on lateral tire slip power losses for different understeer gradients will be presented first in this section. Then, the lateral tire slip power losses will be put in relation to other losses generated during the maneuver such as power losses from the electric drivetrain, longitudinal tire slip losses and total power consumption of the vehicle. As will be seen, the longitudinal tire slip losses are small in comparison with the lateral tire slip losses, but has a significant effect on the power loss reduction obtained through the optimal direct yaw moment.

4.1 Lateral tire slip power losses

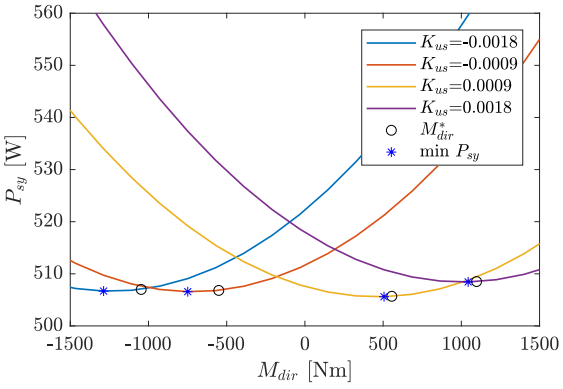

Fig. 2: Lateral slip power losses for different levels of understeer with varying magnitude of direct yaw moment M_{dir} from CarMaker.

In figure 2 the lateral tire slip loss for different applied direct yaw moments is shown for the different understeer gradients. Marked in the figure is also the optimal yaw moments M^*_{dir} according to (16) and the minimum for the lateral tire slip loss, min P_{sy}. The difference between the minimum lateral tire slip loss and the lateral tire slip loss generated with the optimal yaw moment is negligible, thus validating M^*_{dir} as the optimal direct yaw moment. Here, it can be seen that if the vehicle is understeered, i.e. $K_{us} > 0$, a destabilizing direct yaw moment ($M_{dir} > 0$) should be applied to reduce the lateral tire slip loss and a stabilizing yaw moment ($M_{dir} < 0$) should be applied if the vehicle is oversteered. The larger the level of understeer or oversteer, the higher the optimal direct yaw moment is in order to minimize the lateral tire slip losses.

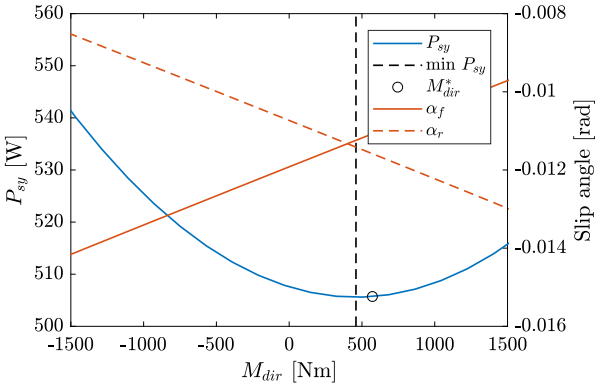

Fig. 3: Lateral tire slip loss and tire slip angles for the understeered case $K_{us} = 0.0009$.

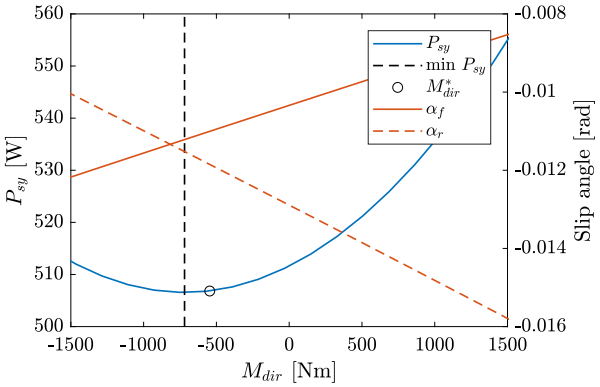

Fig. 4: Lateral tire slip loss and tire slip angles for the oversteered case $K_{us} = -0.0009$.

The lateral tire slip angles presented in figures 3 and 4 are calculated as an average between the right and left tire on each axle. In figure 3, the understeered case with $K_{us} = 0.0009$ is shown. At $M_{dir} = 0$, it can be seen that $|\alpha_f| > |\alpha_r|$, indicating an understeered vehicle, and close to M^*_{dir} they are equal. In the oversteered case with $K_{us} = -0.0009$ in figure 4, the opposite is true with $|\alpha_f| < |\alpha_r|$ indicating an oversteered vehicle, and close to M^*_{dir} they are equal. This supports the claim that by making the vehicle neutralsteered through a direct yaw moment, the lateral tire slip losses are minimized.

Table 3 summarizes the results from the simulation in CarMaker. The optimal direct yaw moment differs slightly between the positive and negative side of the understeer spectrum. This is due to the rounding of the understeer gradient value meaning that they are not exactly mirrored. The percentage of

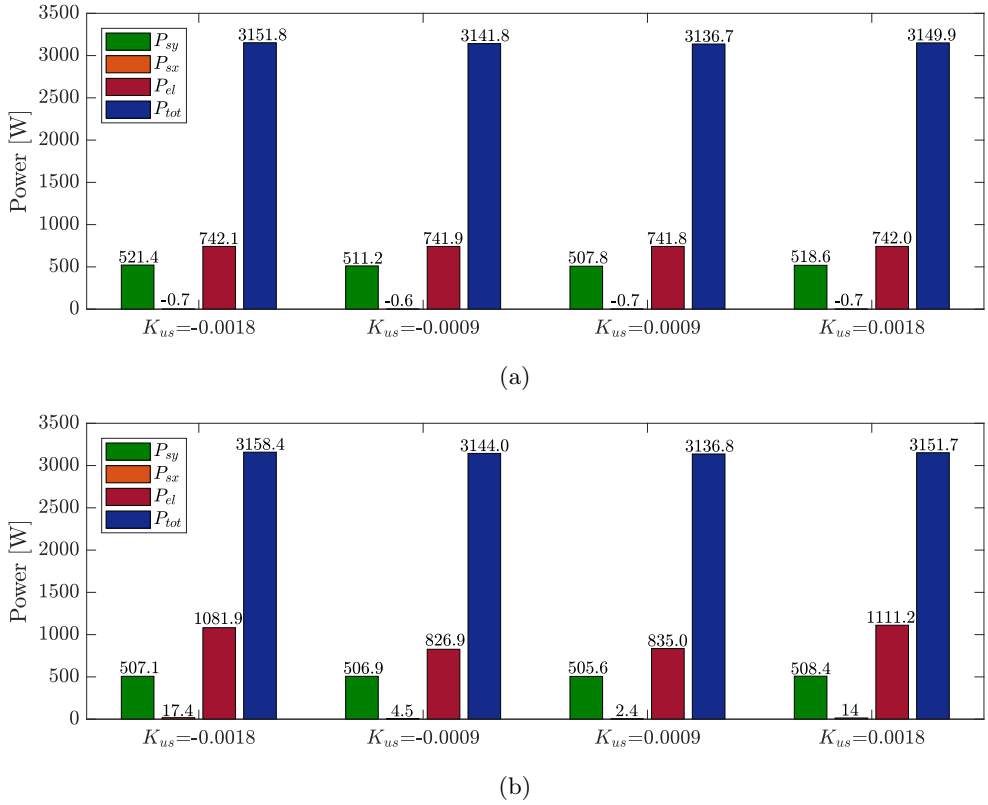

Fig. 5: Comparison between lateral slip losses P_{sy}, electric power losses P_{el}, and total power P_{tot} (excluding electric power losses) for (a) $M_{dir} = 0$ and (b) $M_{dir} = M^*_{dir}$.

lateral tire slip loss that can be reduced increases with increasing levels of understeer or oversteer.

For the two configurations with lower understeer gradients ($K_{us} = -0.0009, K_{us} = 0.0009$), about 0.4-0.9% of the lateral tire slip loss can be reduced by using the optimal yaw moment. As the vehicle becomes more oversteered or more understeered ($K_{us} = -0.0018, K_{us} = 0.0018$), up to 2.9% of the lateral tire slip loss can be reduced. The configurations with lower magnitude of the understeer gradients are closer to neutralsteered, thus the potential for reducing the lateral tire slip loss is smaller. It can thus be concluded that the equation for optimal yaw moment derived using the one-track model works well for models with higher fidelity as it corresponds to minimum values of the lateral tire slip loss and tire slip angles being equal.

4.2 Total power consumption

In figure 5, a comparison between the lateral slip losses, longitudinal slip losses (P_{sx}), electric losses (P_{el}) and total power consumption (P_{tot}), i.e. the power required by the motors (excluding the electric losses) to fulfill the transportation request, can be seen for $M_{dir} = 0$ and $M_{dir} = M^*_{dir}$. The lateral tire slip losses and the electric losses are of similar size, while the total power is about six times higher. In 5a it is seen that the longitudinal tire slip losses are negative, which is most likely due to numerical discrepancies in the tire model defined in CarMaker as power losses cannot be negative.

Comparing 5a and 5b, one can see that the lateral slip losses have reduced in 5b, but the electric losses, longitudinal losses and the total power has increased when applying M^*_{dir}. Although the longitudinal tire slip loss is significantly smaller than the lateral tire slip loss, the decrease in lateral tire slip loss is cancelled by the increase in longitudinal tire slip loss generated through torque vectoring. Hence, the total tire slip loss must be considered. Furthermore, while the lateral slip losses decreased up to 14 W in power when $K_{us} = -0.0018$, the electric losses increased by up to 340 W which is approximately 24 times larger.

4.3 Total tire slip power losses

In figure 6, the total tire slip losses ($P_{s,tot}$) is presented. Comparing this figure to figure 2 which only presented the lateral tire slip power losses, one can see that the total tire slip losses increase at a higher rate as $|M_{dir}|$ increases. The optimal yaw moment M^*_{dir} is now further from the minimum in total tire slip losses, and the difference in $P_{s,tot}$ at M^*_{dir} and $\min P_{s,tot}$ is larger.

In table 4, the minimum total tire slip loss is presented with corresponding direct yaw moment, as well as the decrease in $P_{s,tot}$ and P_{tot} respectively when applying the direct yaw moment that generates the lowest tire slip losses compared to $M_{dir} = 0$. Only focusing on the tire slip losses, the reduction that was seen in the lateral tire slip losses is now less, reaching up to 1.03 % for the most oversteered

Table 4: Minimum total tire slip losses, corresponding direct yaw moment and percentage decrease for $P_{s,tot}$ and P_{tot} compared to $M_{dir} = 0$.

K_{us} [rad/(m/s^2)]	min $P_{s,tot}$ [W]	M_{dir}@min $P_{s,tot}$ [Nm]	$P_{s,tot}$ decrease compared to $M_{dir} = 0$ [%]	P_{tot} decrease compared to $M_{dir} = 0$ [%]
-0.0018	516.1	-448	1.03	0.13
-0.0009	509.3	-244	0.30	0.03
0.0009	505.9	194	0.19	0.04
0.0018	513.2	392	0.77	0.16

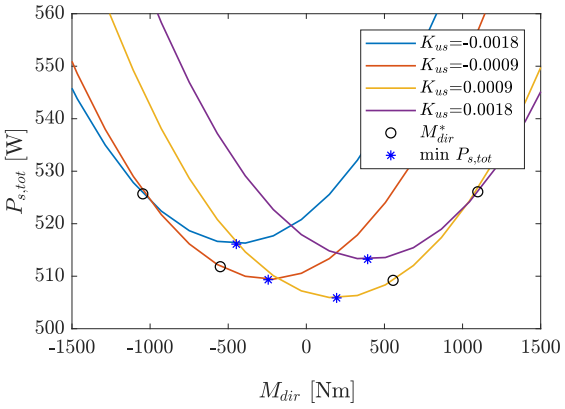

Fig. 6: Total tire slip power losses for different levels of understeer with varying magnitude of direct yaw moment M_{dir} from CarMaker.

case. Looking at the total power consumption, the decrease is even smaller, with a maximum of 0.16 % for the most understeered case.

5. CONCLUSIONS

This work is an optimization and simulation study in which the effect of direct yaw moment on lateral tire slip losses for four vehicle configurations with different understeer levels was investigated. Lateral tire slip losses have been derived for a one-track model, and an expression for the optimal direct yaw moment has been found using a quadratic optimization problem where the objective has been to minimize lateral tire slip losses. The optimal direct yaw moment coincides with the lateral tire slip angles front and rear being equal, indicating that a neutral steering behaviour is optimal. The optimal direct yaw moment was verified using a high fidelity vehicle model in IPG CarMaker by applying a range of direct yaw moments through torque vectoring. It was found that the optimal direct yaw moment is positive for understeered vehicles and negative for oversteered vehicles, and of such magnitude that the vehicle becomes neutralsteered. The larger the understeer or oversteer, the larger the reduction in lateral tire slip loss, here reaching up to 2.9%. However, such a reduction in lateral tire slip loss does not scale to the full vehicle level where the total power is about six times larger than the lateral tire slip losses. Furthermore, longitudinal tire slip losses arise when the direct yaw moment is generated through wheel torque which decreases the total power reduction. By choosing the direct yaw moment that is optimal for the total tire slip loss including both longitudinal and lateral components, up to 0.16% could be saved in the most understeered case which is very little, if not negligible. However, remember that this paper does not study how the vehicle power consumption is affected by torque vectoring through the operating region of the electric motor maps, which can have a much larger effect. Furthermore, the power generated by the steering assist will be affected when applying a direct yaw moment as the driver need to steer less. This will be included in future studies.

REFERENCES

[1] Zhang, X. and Göhlich, D. “Optimal torque distribution strategy for a four motorized wheels electric vehicle”, 28th International Electric Vehicle Symposium and Exhibition, 2015.

[2] Torinsson, J. et al., “Energy reduction by power loss minimisation through wheel torque allocation in electric vehicles: a simulation-based approach.”, Vehicle System Dynamics, 2020.

[3] Kobayashi, T. et al., “Efficient direct yaw moment control: tyre slip power loss minimisation for four-independent wheel drive vehicle”, Vehicle System Dynamics, Vol. 56, No. 5, pp. 719-733, 2018.

[4] Rill, G., “Reducing the cornering resistance by torque vectoring”, Procedia Engineering, No. 199, pp. 3284-3289, 2017.

[5] Parra, A. et al., “On nonlinear model predictive control for energy-efficient torque-vectoring”, IEEE Transactions on Vehicular Technology, Vol. 70, No. 1, pp. 173-188, 2021.

[6] De Filippis, G. et al., “On the Energy Efficiency of Electric Vehicles with Multiple Motors”, Proc. of IEEE Vehicle Power and Propulsion Conference, 2016.

[7] De Filippis, G. et al., “Energy-Efficient Torque-Vectoring Control of Electric Vehicles with Multiple Drivetrains”, IEEE Transactions on Vehicular Technology, Vol. 67, No. 6, pp. 4702-4715, 2018.

[8] Ritchie, M. et al., “A Study of the Relation between Forward Velocity and Lateral Acceleration in Curves During Normal Driving”, Human Factors: The Journal of Human Factors and Ergonomics Society, Vol. 10, No. 3, pp. 255-258, 1968.